IEEE Access
Multidisciplinary | Rapid Review | Open Access Journal

Received August 19, 2019, accepted September 1, 2019, date of publication September 6, 2019,
date of current version September 24, 2019.

*Digital Object Identifier 10.1109/ACCESS.2019.2939837*

# Sequential Optimization of Eco-Driving Taking Into Account Fuel Economy and Emissions

**JINGHUA ZHAO[1,2,3], YUNFENG HU[1,2], AND BINGZHAO GAO[1,2]**
[1]State Key Laboratory of Automotive Simulation and Control, Jilin University Nanling Campus, Changchun 130025, China
[2]Department of Control Science and Engineering, Jilin University Nanling Campus, Changchun 130025, China
[3]Computer College, Jilin Normal University, Siping 136000, China

Corresponding author: Yunfeng Hu (huyf@jlu.edu.cn)

This work was supported in part by the National Natural Science Foundation of China under Grant 61773009, Grant U1864201, and Grant 61703177, in part by the Fundamental Research Funds for the Central Universities, and in part by the Jilin Province Science and Technology Development Plan under Grant 20180101067JC, Grant 20190302105GX, Grant JJKH20180144KJ, Grant JJKH20190999KJ, and Grant 2018C034-5.

**ABSTRACT** The regulations for diesel vehicles are expected to become increasingly more stringent. However, how to coordinate eco-driving, the diesel engine and the urea selective catalytic reduction (urea-SCR) system for fuel economy improvement and emissions reduction remains a formidable challenge. In this paper, a sequential optimization control method with three stages is designed. In stage I, the optimal driving force and braking force are obtained by solving a nonlinear optimization problem of tracking the vehicle velocity profile. In stage II, a real-time reference estimation model is designed to provide the optimal ammonia coverage ratio target. In stage III, to implement the driving force requirement and ammonia coverage ratio target, an integrated engine and urea-SCR system control method and a distributed method are proposed, respectively. The distributed method consists of a fuel injection controller utilizing a data-driven predictive method and a $NH_3$ dosing controller utilizing nonlinear model predictive control (NMPC). The control model of the integrated method is represented by the first-order ammonia coverage ratio dynamics only. The results show that the fuel consumption is improved by 5.3% and the PM emission is reduced by 11.56% during the partial transient acceleration process, and that the fuel consumption and emissions of the integrated control method can accomplish the level of the distributed method and achieve the trade-off between the multi-objective. However, the integrated control method incurs an average computational time penalty of 15.47%.

**INDEX TERMS** Diesel vehicles, urea selective catalytic reduction (urea-SCR) system, sequential optimization, nonlinear model predictive control (NMPC), Pontryagin's minimum principle (PMP).

## I. INTRODUCTION

In recent decades, diesel vehicles are always as the primary commercial transportation instruments because of their well-known high performance in fuel economy and reliability [1]. However, the high $NO_x$ and particulate matter (PM) emissions of diesel vehicles remains a concern [2]. The in-cylinder approaches for improving fuel economy and emissions primarily include the fuel injection mass, start of injection (SOI) and exhaust gas recirculation (EGR). Advancing the SOI timing leads to higher fuel efficiency but inevitably produces higher engine $NO_x$ emission because of the increased in-cylinder temperature [3]. The separate EGR approach is not sufficient to satisfy the increasingly stringent regulations for $NO_x$ emission [4]. Thus, some out-cylinder aftertreatment systems have been added to diesel vehicles to improve fuel economy and reduce emissions. PM emission reduction can be effectively achieved by a diesel particulate filter (DPF) [5]. A urea selective catalytic reduction (urea-SCR) system has shown promising capability for reducing $NO_x$ emission [6], [7]. For the urea-SCR system, when the engine $NO_x$ emission increases rapidly with increasing fuel injection mass, insufficient urea injection results in higher $NO_x$ emission, and urea overdosing in turn can also cause tailpipe ammonia slip. Thus, for simultaneously achieving high fuel efficiency and low $NO_x$ emission, it is necessary to optimize not only the fuel injection but also the ammonia coverage ratio of urea-SCR to fall in the desired range [8]–[10]. Future fuel

The associate editor coordinating the review of this manuscript and approving it for publication was Yue Cao.

  

consumption and emissions testing are expected to be rigorously conducted under real driving emission (RDE) conditions, presenting both a challenge and an opportunity for fuel economy and emissions control. In particular, the urea-SCR system is known to be more advantageous than the lean $NO_x$ trap (LNT) for reducing RDE [11].

Intelligent cruise systems communicating with the Global Positioning System (GPS), Geographical Information System (GIS) and intelligent road traffic systems can offer an optimal velocity trajectory for vehicles [12], [13]. In [14], we proposed a bi-level NMPC methodology [15] utilizing intelligent cruise systems for energy management of hybrid electric vehicles (HEV). The methodology could simplify the hybrid optimal problem and reduce computational time. In the future, cloud-based route optimization systems for intelligent cruise can provide a velocity profile solution for each vehicle in real time. The local controller of vehicle referring the optimal velocity profile and basing on own states of vehicle can further optimize engine and aftertreatment systems. But, some conflicts between the vehicle velocity profile, eco-driving, diesel engine and emissions control are undesirably induced [2], [16]. For example, the accelerating requirements for vehicle velocity result in worse transient emissions because of a rapidly increasing fuel injection mass. In most previous studies, the engine and aftertreatment systems controls were considered separately as two distributed systems [17]. The engine control unit controls torque output and emissions by adjusting the fuel injection, intake air and so forth. When the engine outputs emissions though the urea-SCR system, another control unit adjusts the final exhaust emissions through $NH_3$ dosing. However, the engine and urea-SCR system themselves have a complex coupling relationship with the possibility of integrated control. Integrated control based on a simplified control-oriented model has the potential to reduce the parameter calibration workload and it is expected to benefit engineering applications. However, studies utilizing the simplified integrated control method to achieve a trade-off between the engine and urea-SCR system are scarce. Note that the predictive horizons between the eco-driving, fuel injection and $NH_3$ dosing controls are very different. The predictive horizon in velocity control is normally to the second level, while fuel injection and $NH_3$ dosing are controlled within tens of milliseconds. It is hard to identify the optimal control variables in the typical NMPC optimal problem [18], [19]. Overall, for achieving high fuel efficiency and low emissions, how to coordinate the multi-objective optimal problem remains a formidable challenge.

In this paper, a sequential optimization controller for eco-driving taking into account fuel economy and emissions is proposed, as shown in Fig. 1. The controller against multi-objectives is decoupled into three stages to reduce the computational time and simplify the problem. For evaluating the proposed controller, the scenarios studied assume that a vehicle velocity profile in a certain predictive horizon has been provided by a cloud-based route optimization system. In stage I, for tracking the velocity profile *cyc* provided by the

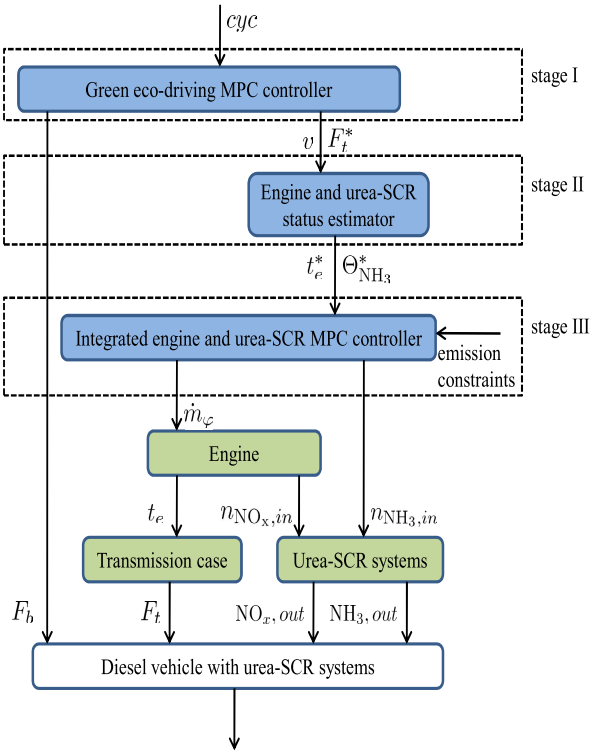


**FIGURE 1.** Sequential optimization algorithm for a diesel vehicle.

cloud-based route optimization systems, the optimal driving force $F_t^*$ and braking force $F_b$ are obtained by solving a eco-driving problem. The nonlinear controller can improve the total fuel consumption and reduce the PM emission during the transient acceleration process. In stage II, a real-time reference estimation model for the urea-SCR status estimates the optimal ammonia coverage ratio target $\Theta_{NH_3}^*$ and engine torque output $\mathcal{T}_e^*$, in accordance with the driving force requirement, engine speed and emission constraints. In stage III, to implement the driving force requirement and ammonia coverage ratio target, an integrated engine and urea-SCR system control method and a distributed method are proposed for adjusting the fuel injection rate $\dot{m}_\varphi$ and $NH_3$ dosing $n_{NH_3,in}$. The distributed method consists of a fuel injection controller utilizing a data-driven predictive method and a $NH_3$ dosing controller utilizing NMPC. The model for the integrated control method is represented by only the first-order ammonia coverage ratio dynamics to avoid a lengthy modeling and parameter calibration process. Under Pontryagin's minimum principle (PMP) framework [20], [21], the eco-driving problem and the integrated engine and urea-SCR system control problem are solved explicitly. Finally, a few simulation verification are preformed to evaluate the system effectiveness in terms of the fuel economy and emissions in the GT-suite/MATLAB environment.

The main merits of the design procedure can be summarized in the following points.

(i) A simplified control-oriented model that includes the vehicle longitudinal dynamics, gearbox, engine and urea-SCR system is developed for a light-duty truck.

(ii) A sequential optimization control method with three stages is designed.

(iii) In stage I, a nonlinear eco-driving problem tracking the optimal velocity profile is solved for reducing the fuel consumption and PM emission.

(iv) In stage II, a real-time reference estimation model is designed to provide the optimal ammonia coverage ratio target.

(v) In stage III, an integrated engine and urea-SCR system control method represented by only the first-order dynamics and a distributed method are proposed and evaluated.

The rest of the paper is organized as follows. In Section II, a simplified dynamic model is developed for a light-duty truck. The sequential optimization control method is designed in Section III. The overall evaluation of the sequential control system is discussed in Section IV. The conclusions are presented in Section V.

## II. MODELING

In this section, a simplified control-oriented model including the vehicle longitudinal dynamics, gearbox, engine and urea-SCR system is developed for a light-duty truck. The model connects vehicle velocity profile tracking, engine torque output, engine emissions and so forth and is the basis for the sequential optimization control method.

### A. CONTROL-ORIENTED VEHICLE LONGITUDINAL DYNAMICS AND GEARBOX MODEL

A vehicle longitudinal dynamics model is developed as:

$$\dot{v} = f_1(v, F_t, F_b) = \frac{1}{M}(F_t - F_b - \frac{1}{2}\rho c_d A_f v^2) - c_r g, \quad (1)$$

where $v$ is the vehicle velocity, $M$ is the equivalent mass, $F_t$ is the driving force transmitted through engine torque, $F_b$ is the braking force, $\frac{1}{2}\rho c_d A_f$ is the aerodynamic drag resistance, and $c_r g$ represents the acceleration caused by the rolling resistance and the gradient resistance, which is determined by the road slope $\alpha$, as

$$c_r = \beta \cos(\alpha(s)) + \sin(\alpha(s)). \quad (2)$$

Based on rule-based control, a six speed gearbox model is developed without considering energy-saving optimization strategies. As implemented through the gearbox, the relationship between the engine torque $\mathcal{T}_e$ and $F_t$ can be expressed as $\mathcal{T}_e = F_t r/\eta_t i_0\, i_g$, and the relationship between the engine speed $\omega_e$ and $v$ can be expressed as $\omega_e = 30\, i_0\, i_g v/r\pi$. The nomenclature of the constants used in the modeling are shown in Table 1.

**TABLE 1. Vehicle parameters.**

| symbol | description | value[unit] |
|---|---|---|
| $M$ | Vehicle mass | 3000 [kg] |
| $\rho$ | Air density | 1.205 [kg.m$^{-3}$] |
| $A_f$ | Face area | 4[m$^2$] |
| $c_d$ | Coefficient of air resistance | 0.5 |
| $i_0$ | Final drive speed ratio | 5.00 |
| $\beta$ | Coefficient of rolling resistance | 0.011 |
| $\eta_t$ | Drive train total efficiency | 0.96 |
| $r$ | Dynamic tire radius | 0.51 [m] |
| $i_g$ | gear ratio | - |
| $i_{g1}$ | First gear ratio | 6.67 |
| $i_{g2}$ | Second gear ratio | 4.10 |
| $i_{g3}$ | Third gear ratio | 2.42 |
| $i_{g4}$ | Fourth gear ratio | 1.52 |
| $i_{g5}$ | Fifth gear ratio | 1 |
| $i_{g6}$ | Sixth gear ratio | 0.78 |

### B. CONTROL-ORIENTED ENGINE MODEL

A simplified control-oriented model for an engine is adopted. Diesel engines are complex dynamic systems with highly nonlinear sub-components [22]. To keep the focus on the control design of the fuel injection and urea-SCR system, the influences of EGR and SOI on fuel consumption and emissions are considered negligible. Moreover, a single-injection strategy is adopted from the fuel economy viewpoint.

Based on a large number of experimental data analyses, the relationship between parameters of the engine can be briefly described by some fitting formulas [23]. Employing these quadratic regression and fitting methods, a simplified model of $\mathcal{T}_e$, $T_{exhaust}$, $m^*_{\mathrm{EG}}$ and $m_{\mathrm{NO}_x}$ can be presented by the following equation. With reference to the current engine speed $\omega_e$, the engine torque $\mathcal{T}_e$ is influenced mainly by the fuel injection rate $\dot{m}_\varphi$, as shown in (3a). The exhaust gas temperature $T_{exhaust}$ is influenced mainly by the engine power, which is determined by the product of $\omega_e$ and $\mathcal{T}_e$, as shown in (3b). The exhaust gas mass flow $m^*_{\mathrm{EG}}$ is influenced mainly by $\omega_e$, as shown in (3c). The engine $\mathrm{NO}_x$ emission $m_{\mathrm{NO}_x}$ is influenced mainly by $\dot{m}_\varphi$, as shown in (3d).

$$\mathcal{T}_e = f_t(\dot{m}_\varphi, \omega_e) = \frac{b_2 + \dot{m}_\varphi}{b_1 \omega_e}, \quad (3a)$$

$$T_{exhaust} = f_T(\mathcal{T}_e, \omega_e) = b_5 \mathcal{T}_e \omega_e + b_6, \quad (3b)$$

$$m^*_{\mathrm{EG}} = f_{mEG}(\omega_e) = b_7 \omega_e + b_8, \quad (3c)$$

$$m_{\mathrm{NO}_x} = f_c(\dot{m}_\varphi) = b_4 + b_3 \dot{m}_\varphi, \quad (3d)$$

where $b_i, (i = 1, 2, \ldots, 8)$ are calibrated parameters. All nomenclature of the variables used in the modeling is shown in Table 2.

The experimental data for calibration analysis derive from the European Transient Cycle (ETC), whose total cycle time is 1800 s and includes three typical conditions, namely, urban areas, suburbs and highway. As shown in Fig. 2, the urban area conditions are selected as a training data-set for parameter calibration. These transient conditions variy strongly enough to be useful in calibration. As shown in Fig. 3, the parameter values of equation (3) are calibrated and are listed in Table 4 of Appendix Section V.

The transient data are also sufficient for subspace identification of the data-driven model predictive control (DDMPC)

**TABLE 2. Variable nomenclature of the engine and urea-SCR system.**

| symbol | description/unit |
|---|---|
| $\mathcal{T}_e$ | Engine torque [Nm] |
| $T_{exhaust}$ | Exhaust gas temperature of engine [K] |
| $m^*_{\mathrm{EG}}$ | Exhaust gas mass flow [kg. $\mathrm{s}^{-1}$] |
| $m_x$ | Mass flow of species x [kg. $\mathrm{h}^{-1}$] |
| $\omega_e$ | Engine speed [r. $\mathrm{min}^{-1}$] |
| $\dot{m}_\varphi$ | Fuel injection rate [kg. $\mathrm{h}^{-1}$], |
| $m_\varphi$ | Fuel injection mass [mg. $\mathrm{hub}^{-1}$] |
| $C_x$ | Molar concentration of species x[mol. $\mathrm{m}^{-3}$] |
| $n_x$ | Molar mass flow of species x[mol. $\mathrm{s}^{-1}$] |
| $T_{\mathrm{amb}}$ | Ambient temperature [K] |
| $T_{\mathrm{SCR}}$ | Gas temperature in urea-SCR [K] |
| $\Theta_{\mathrm{NH_3}}$ | Scaled surface coverage with $\mathrm{NH_3}$ [-] |

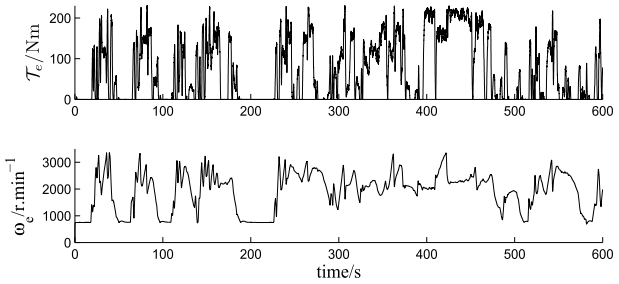


**FIGURE 2. Engine torque and speed of the ETC cycle.**

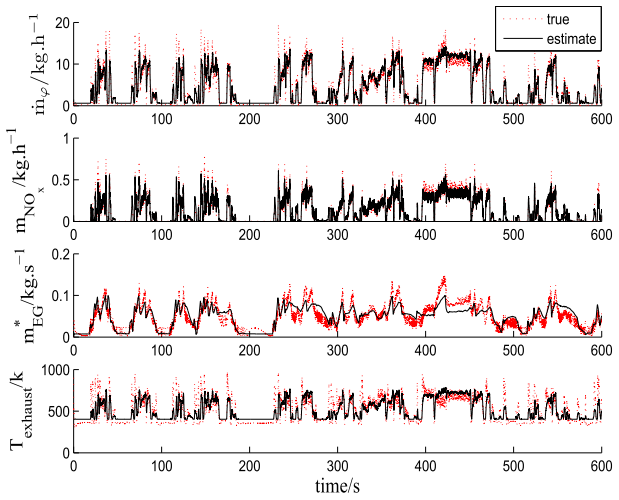


**FIGURE 3. Calibration result of the engine estimation model.**

method [24]. Utilizing the DDMPC method, another controller for comparison verification is designed in Section III.

### C. CONTROL-ORIENTED UREA-SCR SYSTEM MODEL

A simplified control-oriented model for the urea-SCR system is adopted. The chemical reaction modeling process, as described in the literature [9], is based on the assumption that the catalyst is a continuously stirred tank reactor (CSTR) and that all the species in the catalyst (reactor) are homogeneous. Based on the assumption and the mass balance and heat balance, the ordinary differential equations (ODEs) of the 1-cell urea-SCR catalyst dynamic model can be described as (4), as shown at the bottom of the next page, where the parameters are defined as (5), as shown at the bottom of the next page.

In addition, the relationship $n_{x,in} = a_0 m^*_{\mathrm{EG}} T_{\mathrm{SCR}} C_{\mathrm{x}}$ pertains between the molar concentration and molar mass flow. Thus, in the urea-SCR system, the $\mathrm{NO}_x$ concentration can be described as

$$C_{\mathrm{NO}_x} = f_c(\dot{m}_\varphi, m^*_{\mathrm{EG}}, T_{exhaust}) = \frac{0.0099 \times (b_4 + b_3 \dot{m}_\varphi)}{a_0 m^*_{\mathrm{EG}} T_{exhaust}}. \tag{6}$$

The 1-cell model presented here refers to the assumptions and simplifications in [25], [26]. All nomenclature of the constants and variables used in the modeling is shown in Table 2 and 3.

## III. SEQUENTIAL OPTIMIZATION

In this section, a sequential optimization control method is designed to coordinate eco-driving, the diesel engine and the urea-SCR system for fuel economy improvement and emissions reduction. In stage I, the optimal driving force and braking force are obtained by solving a nonlinear eco-driving problem tracking the vehicle velocity profile. In stage II, a real-time reference estimation model is designed to provide the optimal ammonia coverage ratio target. In stage III, to implement the driving force requirement and ammonia coverage ratio target, an integrated engine and urea-SCR system control method and a distributed method are proposed.

### A. STAGE I: ECO-DRIVING OPTIMIZATION CONTROL

In this subsection, the nonlinear eco-driving problem of tracking the vehicle velocity profile *cyc* provided by the cloud-based route optimization system is solved. Simultaneously, the method can reduce the fuel consumption and PM emission. In this optimization problem, the state is selected as $v$, and the control inputs are $F_t$ and $F_b$. The optimal control problem can be formulated as

$$\begin{aligned} &\min J_1 = \varphi_1(v(t+T)) + \int_t^{t+T} L_1(v, F_t, F_b, t')dt', \\ &s.t.\ \dot{v}(t) = \frac{1}{M}(F_t(t) - F_b(t) - \frac{1}{2}\rho c_d A_f v^2(t)) - c_r g, \end{aligned} \tag{7}$$

where $t' \in [t, t+T]$. During the acceleration of the diesel vehicle, how to find a trade-off between the accelerating requirements, fuel consumption and PM emission remains a formidable challenge. Thus, the cost function $L_1$ is formulated as:

$$\begin{aligned} L_1(v, F_t, F_b, t) = \omega_t (F_t(t)v(t))^2 + \omega_b F_b^2(t) + \omega_d (F_t(t+1) \\ - F_t(t))^2 + \omega_v (v(t) - cyc(t))^2, \end{aligned} \tag{8}$$

where the cost related to the fuel consumption $(F_t(t)v(t))^2$ is multiplied by a weight $\omega_t$, the brake force $F_b^2(t)$ is weighted

**TABLE 3.** Constant nomenclature of the urea-SCR system.

| symbol | description | value/unit |
|---|---|---|
| $S_c$ | Area of one molar of the active surface atoms | 581[$m^2$/mol] |
| $\alpha_{\text{prob}}$ | Sticking probability | 1.11e-3[-] |
| $c_s$ | Concentration of active surface atoms with respect to the converter gas volume | 7.30[mol/$m^3$ ] |
| $c_{\text{p,EG}}$ | Specific heat at constant pressure of the exhaust gas | 1060 [J/kgK ] |
| $c_{\text{p,c}}$ | Specific heat of the catalysts | 1054[J/kgK] |
| $M_{\text{NH}_3}$ | Molar mass of $NH_3$ | 17 [g/mol] |
| $R$ | Universal gas constant | 8.3145 [J/molK] |
| $R_{\text{S,EG}}$ | Gas constant of the engine | 288 [J/kgK] |
| $k_{\text{Des}}$ | Pre-exponential factor of desorption | 0.514 [1/s] |
| $k_{\text{SCR}}$ | Pre-exponential factor of urea-SCR | 2.6776[$m^2$/s] |
| $k_{\text{Ox}}$ | Pre-exponential factor of $NH_3$ oxidation | 3.34e6[1/s] |
| $E_{a,\text{ Des}}$ | Activation energy of desorption | 15.2 [J/mol] |
| $E_{a,\text{ SCR}}$ | Activation energy of urea-SCR | 28471[J/mol] |
| $E_{a,\text{ Ox}}$ | Activation energy of $NH_3$ oxidation | 1.16e5[J/mol] |
| $P_{\text{amb}}$ | Ambient pressure | 101325[Pa] |
| $V_c$ | Total volume of the urea-SCR system | 0.01 [$m^3$] |
| $m_c$ | Mass of the catalytic converter | 19[kg] |
| $\varepsilon$ | Ratio of gas to total converter volume | 0.81[-] |
| $\varepsilon_{\text{rad,scr}}$ | Radiation coefficient of silencer | 0.507[-] |
| $\sigma_{\text{sb}}$ | Radiation constant | 5.67e-8[-] |
| $A_{\text{rad,scr}}$ | Radiating surface area of the silencer | 0.9044[$m^2$] |

by $\omega_b$ to avoid unnecessary braking, the change rate of the driving force $(F_t(t+1)-F_t(t))^2$ is weighted by $\omega_d$ to avoid PM emission deterioration resulting from rapid acceleration and to improve the ride comfortability, and the velocity trajectory tracking $(v(t)-cyc(t))^2$ is weighted by $\omega_v$ [16]. In particular, the existence of $\omega_d(F_t(t+1)-F_t(t))^2$ is important for fuel consumption and transient PM emission controls. The constraints in the optimal problem (7) are given as follows:

$$\begin{aligned}\varphi_1(v(t+T)) &= \kappa_1(v(t+T)-cyc(t+T))^2,\\ v_{min} &\le v(t) \le v_{max},\\ F_{t,min} &\le F_t(t) \le F_{t,max}, 0 \le F_b(t) \le F_{b,max},\end{aligned} \quad (9)$$

where $v_{min}$ and $v_{max}$ are velocity limits, $F_{t,min}$ and $F_{t,max}$ are driving force limits, and $F_{b,max}$ is a braking force limit.

### B. STAGE II: REAL-TIME REFERENCE ESTIMATION MODEL FOR THE AMMONIA COVERAGE RATIO TARGET

In this subsection, a real-time reference estimation model for the optimal ammonia coverage ratio target is designed in accordance with the driving force requirement, engine speed and emission constraints. The derivation process of the optimal ammonia coverage ratio target $\Theta^*_{\text{NH}_3}$ is shown in Fig. 4. The eco-driving problem is solved to obtain the optimal driving force $F_t^*$ (the control input $F_t$ of the optimization problem (7)) and actual vehicle velocity $v$. Through analysis of the six speed gearbox, the engine torque requirements $\mathcal{T}_e^*$ and engine speed $\omega_e$ can be obtained. Thus, all input parameters required for the urea-SCR system operation, including $m_{\text{NO}_x}$, $T_{exhaust}$ and $m^*_{\text{EG}}$, can be obtained by the calibration relationships shown as equation (3). Finally,

$$\dot{C}_{\text{NO}_x} = a_1 n_{\text{NO}_x,in} - C_{\text{NO}_x}(a_0 a_1 m^*_{\text{EG}} T_{\text{SCR}} + a_4(T_{\text{SCR}})\Theta_{\text{NH}_3}), \quad (4a)$$

$$\dot{C}_{\text{NH}_3} = a_1 n_{\text{NH}_3,in} - C_{\text{NH}_3}[a_0 a_1 m^*_{\text{EG}} T_{\text{SCR}} + a_2(T_{\text{SCR}})(1-\Theta_{\text{NH}_3})] + a_3(T_{\text{SCR}})\Theta_{\text{NH}_3}, \quad (4b)$$

$$c_s\dot{\Theta}_{\text{NH}_3} = a_2(T_{\text{SCR}})(1-\Theta_{\text{NH}_3})C_{\text{NH}_3} - [a_3(T_{\text{SCR}}) + a_4(T_{\text{SCR}})C_{\text{NO}_x} + a_5(T_{\text{SCR}})]\Theta_{\text{NH}_3}, \quad (4c)$$

$$\dot{T}_{\text{SCR}} = a_6 m^*_{\text{EG}}(T_{exhaust} - T_{\text{SCR}}) - a_7(T^4_{\text{SCR}} - T^4_{\text{amb}}), \quad (4d)$$

$$a_0 = \frac{R_{\text{S,EG}}}{P_{\text{amb}}}, \quad a_1 = \frac{1}{\varepsilon V_c}, \; a_2(T_{\text{SCR}}) = c_s S_c \alpha_{\text{Prob}}\sqrt{\frac{RT_{\text{SCR}}}{2\pi M_{\text{NH}_3}}}, \; a_3(T_{\text{SCR}}) = c_s k_{\text{Des}} e^{\left(\frac{-E_{a,\text{ Des}}}{RT_{\text{SCR}}}\right)}, \quad (5a)$$

$$a_4(T_{\text{SCR}}) = c_s R T_{\text{SCR}} k_{\text{SCR}} e^{\left(\frac{-E_{a,\text{ SCR}}}{RT_{\text{SCR}}}\right)}, \quad a_5(T_{\text{SCR}}) = c_s k_{\text{Ox}} e^{\left(\frac{-E_{a,\text{Ox}}}{RT_{\text{SCR}}}\right)}, \; a_6 = \frac{c_{\text{p,EG}}}{c_{\text{p,c}} m_c}, \; a_7 = \frac{\varepsilon_{\text{rad,scr}}\sigma_{\text{sb}} A_{\text{rad,scr}}}{c_{\text{p,c}} m_c}. \quad (5b)$$

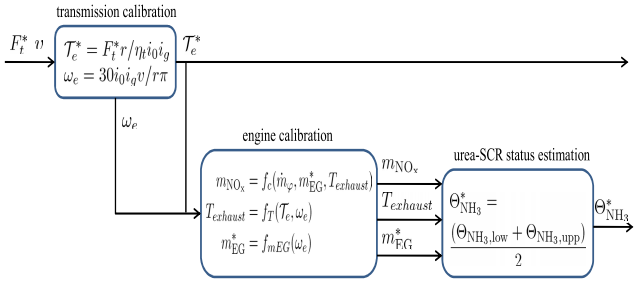


**FIGURE 4.** Real-time reference estimation for ammonia coverage ratio target.

$\Theta^*_{\mathrm{NH_3}}$ can be obtained through the following derivation process.

For simultaneously achieving high $\mathrm{NO}_x$ conversion efficiency and low ammonia slip, the controller must maintain $\Theta^*_{\mathrm{NH_3}}$ within a reasonable region. In this subsection, $\Theta^*_{\mathrm{NH_3}}$ are provided as the average of the upper bound and lower bound of this parameter. It is assumed that an effective thermal management method for the urea-SCR system is used such that the upper bound is always greater than the lower bound. A simple method of obtaining the upper bound $\Theta_{\mathrm{NH_3,upp}}$ and lower bound $\Theta_{\mathrm{NH_3,low}}$ [27] based on the emission constraints is introduced in the following content.

In the simplified urea-SCR model (4), the $\mathrm{NO}_x$ and $\mathrm{NH_3}$ concentration dynamics are much faster than the ammonia coverage ratio dynamics. Thus, equation (4a) and equation (4b) based on the singular perturbation method are degenerated into the following two equations:

$$0 = a_1 n_{\mathrm{NO}_x,in} - C_{\mathrm{NO}_x}(a_0 a_1 m^*_{\mathrm{EG}} T_{\mathrm{SCR}} + a_4(T_{\mathrm{SCR}})\Theta_{\mathrm{NH_3}}), \tag{10}$$

$$0 = a_1 n_{\mathrm{NH_3},in} - C_{\mathrm{NH_3}}[a_0 a_1 m^*_{\mathrm{EG}} T_{\mathrm{SCR}} + a_2(T_{\mathrm{SCR}})(1 - \Theta_{\mathrm{NH_3}})] + a_3(T_{\mathrm{SCR}})\Theta_{\mathrm{NH_3}}. \tag{11}$$

In this subsection, an emission constraint is proposed such that the $\mathrm{NO}_x$ conversion efficiency is $\xi_{nox}\%$, which can be adjusted in real time in accordance with the emission requirements of RDE conditions. In other words, the following inequality should be satisfied according to (10):

$$C_{\mathrm{NO}_x} = \frac{a_1 n_{\mathrm{NO}_x,in}}{(a_0 a_1 m^*_{\mathrm{EG}} T_{\mathrm{SCR}} + a_4(T_{\mathrm{SCR}})\Theta_{\mathrm{NH_3}})} < C_{\mathrm{NO}_x,d}, \tag{12}$$

where the time-varying threshold $C_{\mathrm{NO}_x,d}$ is designed as $(1 - \xi_{nox}\%)$ of the engine $\mathrm{NO}_x$ emission $n_{\mathrm{NO}_x,in}$.

The lower ammonia coverage ratio $\Theta_{\mathrm{NH_3,low}}$ is obtained according to (12)

$$\Theta_{\mathrm{NH_3,low}}(\eta_{\mathrm{NO}_x}, m^*_{\mathrm{EG}}, T_{\mathrm{SCR}}) = \frac{a_1 \eta_{\mathrm{NO}_x} - a_0 a_1 m^*_{\mathrm{EG}} T_{\mathrm{SCR}}}{a_4(T_{\mathrm{SCR}})}, \tag{13}$$

where $\eta_{\mathrm{NO}_x} = \frac{n_{\mathrm{NO}_x,in}}{C_{\mathrm{NO}_x,d}} = 100/(100 - \xi_{nox})$. In this paper, this variable $\xi_{nox}$ takes a constant value of 90.

The following equality can be derived according to (11):

$$\Theta_{\mathrm{NH_3,upp}}(C_{\mathrm{NH_3},d}, m^*_{\mathrm{EG}}, T_{\mathrm{SCR}}) = \frac{C_{\mathrm{NH_3},d}(a_0 a_1 m^*_{\mathrm{EG}} T_{\mathrm{SCR}} + a_2(T_{\mathrm{SCR}})) - a_1 n_{\mathrm{NH_3},in}}{a_3(T_{\mathrm{SCR}}) + a_2(T_{\mathrm{SCR}}) C_{\mathrm{NH_3},d}}. \tag{14}$$

Another constraint is that the tailpipe ammonia slip must be less than a constant threshold $C_{\mathrm{NH_3},d} = \xi_{nh3}$ ppm, which can also be adjusted in real time in accordance with the emission requirements of the RDE conditions. In this paper, this variable $\xi_{nh3}$ takes a constant value of 24.

Finally, the reference values of the ammonia coverage ratio

$$\Theta^*_{\mathrm{NH_3}} = \frac{(\Theta_{\mathrm{NH_3,low}} + \Theta_{\mathrm{NH_3,upp}})}{2} \tag{15}$$

are provided as the average of the upper bound and lower bound constraints.

### C. STAGE III: ENGINE AND UREA-SCR SYSTEM CONTROL

In accordance with the engine torque requirements $\mathcal{T}_e^*$ and the optimal ammonia coverage ratio target $\Theta^*_{\mathrm{NH_3}}$, an integrated engine and urea-SCR system control method and a distributed method are proposed for the explicit solutions of the fuel injection mass and $\mathrm{NH_3}$ dosing. The both proposed methods are based on the same set of transient data (shown in Fig. 2 and Fig. 3).

#### 1) INTEGRATED ENGINE AND UREA-SCR SYSTEM CONTROL

An integrated engine and urea-SCR system controller is designed, as shown in Fig. 5. First, a simplified first-order dynamic model, including the engine and urea-SCR system, is developed. Substituting (6) into (4c) with unit conversion leads to

$$\begin{aligned}\dot{\Theta}_{\mathrm{NH_3}} &= f_2(\Theta_{\mathrm{NH_3}}, \dot{m}_\varphi, n_{\mathrm{NH_3},in}) \\ &= \frac{1}{c_s}[a_2(T_{\mathrm{SCR}})(1 - \Theta_{\mathrm{NH_3}})\frac{n_{\mathrm{NH_3},in}}{a_0 m^*_{\mathrm{EG}} T_{\mathrm{SCR}}} - [a_3(T_{\mathrm{SCR}}) \\ &\quad + a_4(T_{\mathrm{SCR}})((b_4 + b_3\dot{m}_\varphi)a_8) + a_5(T_{\mathrm{SCR}})]\Theta_{\mathrm{NH_3}}],\end{aligned} \tag{16}$$

where $a_8 = \frac{0.0099}{a_0 m^*_{\mathrm{EG}} T}$. The model represents by the first-order ammonia coverage ratio dynamics only and omits many modeling and parameter calibration processes. The model is suitable for solving optimization problems in industrial applications.

In this integrated engine and urea-SCR system optimization problem, the state is selected as $\Theta_{\mathrm{NH_3}}$. In the predictive horizon $[t, t+\Delta\tau]$, the objective is to find the optimal control law $\dot{m}_\varphi$, $n_{\mathrm{NH_3},in}$ for tracking $\Theta^*_{\mathrm{NH_3}}$ and $\mathcal{T}_e^*$ under the emission constrains. The law can minimize the fuel consumption and maintain a relatively higher $\mathrm{NO}_x$ conversion efficiency without increasing the tailpipe ammonia slip. Thus, the cost function derived for the integrated control method is expressed in

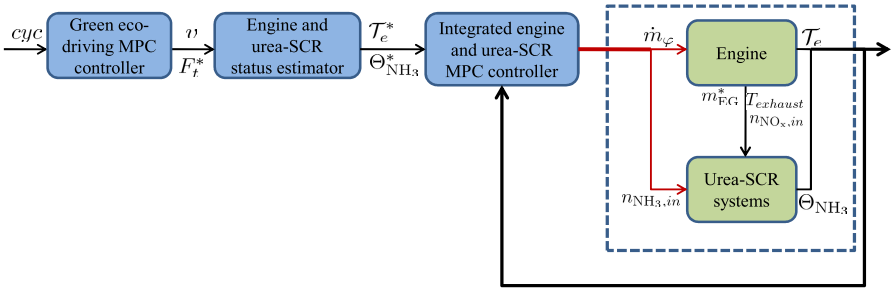


**FIGURE 5.** Control diagram of integrated engine and urea-SCR system control.

the following equation:

$$\begin{aligned}
&\min J_2 = \varphi_2(\Theta_{NH_3}(t+\Delta\tau), \mathcal{T}_e(t+\Delta\tau)) \\
&\quad + \int_t^{t+\Delta\tau} L_2(\Theta_{NH_3}, \mathcal{T}_e, \dot{m}_\varphi, t')dt', \\
&s.t.\ \dot{\Theta}_{NH_3}(t) = \frac{1}{c_s}[a_2(T_{SCR})(1-\Theta_{NH_3}(t))\frac{n_{NH_3,in}(t)}{a_0 m_{EG}^*(t) T_{SCR}} \\
&\quad - [a_3(T_{SCR}) + a_4(T_{SCR})((b_4 + b_3\dot{m}_\varphi(t))a_8) \\
&\quad + a_5(T_{SCR})]\Theta_{NH_3}(t)], \qquad (17)
\end{aligned}$$

where $L_2(\Theta_{NH_3}, \mathcal{T}_e, \dot{m}_\varphi, t) = \phi_\theta(\Theta_{NH_3}^*(t) - \Theta_{NH_3}(t))^2 + \phi_T(\mathcal{T}_e^*(t) - \mathcal{T}_e(t))^2 + \phi_m(\gamma_f \dot{m}_\varphi(t))^2$, $\gamma_f$ denote the cost of diesel fuel, the tracking for the ammonia coverage ratio target $(\Theta_{NH_3}^*(t) - \Theta_{NH_3}(t))^2$ is weighted by $\phi_\theta$, the tracking for the torque target $(\mathcal{T}_e^*(t) - \mathcal{T}_e(t))^2$ is weighted by $\phi_T$, and the fuel consumption $(\gamma_f \dot{m}_\varphi(t))^2$ is weighted by $\phi_m$. The constraints in the optimization problem (17) are given as follows:

$$\begin{aligned}
&\varphi_2(\Theta_{NH_3}(t+\Delta\tau), \mathcal{T}_e(t+\Delta\tau)) \\
&\quad = \kappa_2(\Theta_{NH_3}^*(t+\Delta\tau) - \Theta_{NH_3}(t+\Delta\tau))^2 \\
&\quad\quad + \kappa_3(\mathcal{T}_e^*(t+\Delta\tau) - \mathcal{T}_e(t+\Delta\tau))^2, \\
&0 \le \Theta_{NH_3}(t) \le 1, \\
&0 \le \dot{m}_\varphi(t) \le \dot{m}_{\varphi,max}, \\
&0 \le n_{NH_3,in}(t) \le n_{NH_3,in,max}, \qquad (18)
\end{aligned}$$

where $\dot{m}_{\varphi,max}$ is the fuel injection rate limit, and $n_{NH_3,in,max}$ is the $NH_3$ dosing limit. In the integrated optimization problem, solving the trade-off between these multi-objectives can be achieved through the adjustment of several weighting factors.

The solutions for the optimization problems (7) and (17) are discussed in this section. An indirect method based on PMP is used to find an optimal solution that can be implementable in real time. Divide the horizon into $N = T/\Delta\tau$ steps, and discretize the optimal control problem (7) on the sampling time $\Delta\tau$-axis with the forward difference as follows:

$$\begin{aligned}
&\min J_1 = \varphi_1(v(N)) + \sum_{k=0}^{N-1} L_1(v(k), F_t(k), F_b(k))\Delta\tau, \\
&s.t.\ v(k+1) = v(k) + f_1(v(k), F_t(k), F_b(k))\Delta\tau. \qquad (19)
\end{aligned}$$

Divide the horizon into $n = \Delta\tau/\Delta t$ steps, and discretize the optimal control problem (17) on the sampling time $\Delta t$-axis with the forward difference as follows:

$$\begin{aligned}
&\min J_2 = \varphi_2(\Theta_{NH_3}(N), \mathcal{T}_e(N)) \\
&\quad + \sum_{k=0}^{n-1} L_2(\Theta_{NH_3}(k), \mathcal{T}_e(k), \dot{m}_\varphi(k))\Delta t, \\
&s.t.\ \Theta_{NH_3}(k+1) = \Theta_{NH_3}(k) \\
&\quad + f_2(\Theta_{NH_3}(k), \dot{m}_\varphi(k), n_{NH_3,in}(k))\Delta t. \qquad (20)
\end{aligned}$$

For the optimization problem (19), the Hamiltonian in discrete time is defined to be

$$\begin{aligned}
&H_1(v(k), F_t(k), F_b(k), \lambda_1(k+1)) \\
&= L_1(v(k), F_t(k), F_b(k)) + \lambda_1(k+1)(\frac{v(k+1)-v(k)}{\Delta\tau})\Delta\tau \\
&= \omega_t(F_t(k)v(k))^2 + \omega_b F_b^2(k) \\
&\quad + \omega_d(F_t(k+1) - F_t(k))^2 + \omega_v(v(k) - cyc(k))^2 \\
&\quad + \lambda_1(k+1)(\frac{1}{M}(F_t(k) - F_b(k) - \frac{1}{2}\rho c_d A_f v^2(k)) - c_r g)\Delta\tau. \qquad (21)
\end{aligned}$$

Substituting (3) into the optimization problem (20), the Hamiltonian in discrete time is defined to be

$$\begin{aligned}
&H_2(\Theta_{NH_3}(k), \dot{m}_\varphi(k), n_{NH_3,in}(k), \lambda_2(k+1)) \\
&\quad = L_2(\Theta_{NH_3}(k), \mathcal{T}_e(k), \dot{m}_\varphi(k)) \\
&\quad\quad + \lambda_2(k+1)(\frac{\Theta_{NH_3}(k+1) - \Theta_{NH_3}(k)}{\Delta t})\Delta t \\
&\quad = \phi_\theta(\Theta_{NH_3}(k) - \Theta_{NH_3}^*(k))^2 + \phi_T(\mathcal{T}_e^*(k) \\
&\quad\quad - (\frac{b_2 + \dot{m}_\varphi(k)}{b_1\omega_e}))^2 + \phi_m(\gamma_f \dot{m}_\varphi(k))^2 \\
&\quad\quad + \frac{\lambda_2(k+1)\Delta t}{c_s}[a_2(1 - \Theta_{NH_3}(k))\frac{n_{NH_3,in}}{a_0 m_{EG}^* T} \\
&\quad\quad - [a_3 + a_4(b_4 + b_3\dot{m}_\varphi(k))a_8 + a_5]\Theta_{NH_3}(k)]. \qquad (22)
\end{aligned}$$

The costate variables are described as $\lambda_1(k+1)$ and $\lambda_2(k+1)$. PMP states that the optimal control input $u_1$ and $u_2$ must satisfy:

$$\begin{aligned}
&H_1(v^*(k), \lambda_1^*(k+1), F_t^*(k), F_b^*(k)) \\
&\quad \le H_1(v^*(k), \lambda_1^*(k+1), F_t(k), F_b(k)), \\
&k \in [0, 1, \cdots, N-1], \\
&\quad H_2(\Theta_{NH_3}^*(k), \lambda_2^*(k+1), \dot{m}_\varphi^*(k), n_{NH_3,in}^*(k)) \\
&\quad \le H_2(\Theta_{NH_3}^*(k), \lambda_2^*(k+1), \dot{m}_\varphi(k), n_{NH_3,in}(k)), \\
&k \in [0, 1, \cdots, N-1], \qquad (23)
\end{aligned}$$

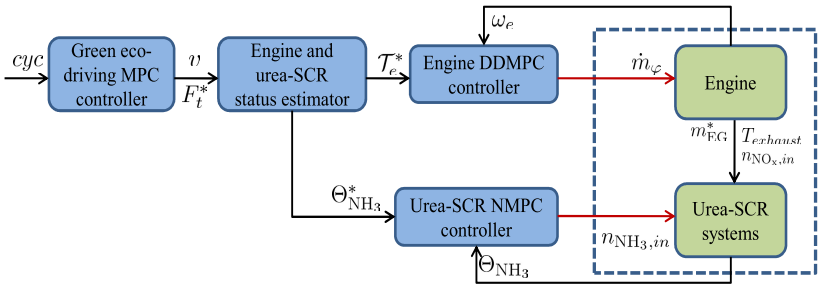


**FIGURE 6.** Control diagram of the distributed engine and urea-SCR system control.

where $v^*(k) \in \Omega_1[0, 1, \cdots, N-1]$ is the optimal trajectory of the vehicle speed, $\lambda_1^*(k+1) \in \Omega_2[0, 1, \cdots, N-1]$ is the optimal trajectory of its costate variable, $\Theta_{NH_3}^*(k) \in \Omega_2[0, 1, \cdots, N-1]$ is the optimal trajectory of the ammonia coverage ratio, and $\lambda_2^*(k+1) \in \Omega_2[0, 1, \cdots, N-1]$ is the optimal trajectory of its costate variable. In addition, the equations of the costate variables are given as

$$\begin{aligned}
&\lambda_1(k+1)\\
&= -\frac{\partial H_1(v(k), F_t(k), F_b(k), \lambda_1(k+1))}{\partial v(k)} + \lambda_1(k)\\
&= 2v(k)(\omega_t F_t^2(k) + \omega_v - \lambda_1(k+1)\Delta\tau\frac{\rho c_d A_f}{2M})\\
&\quad - 2\omega_v cyc(k) + \lambda_1(k),\\
&\lambda_1(N)\\
&= 2\kappa_1(v(N) - cyc(N)),\\
&\quad \lambda_2(k+1)\\
&= -\frac{\partial H_2(\Theta_{NH_3}(k), \dot{m}_\varphi(k), n_{NH_3,in}(k), \lambda_2(k+1))}{\partial \Theta_{NH_3}(k)} + \lambda_2(k)\\
&= \phi_\theta - \frac{1}{c_s}a_4 b_3 a_8 \lambda_2(k+1)\Delta t \dot{m}_\varphi(k)\\
&\quad - \frac{1}{c_s}\lambda_2(k+1)\Delta t(a_3 + a_4 b_4 a_8 + a_5)\\
&\quad - \frac{1}{c_s}\lambda_2(k+1)\Delta t a_2 \frac{n_{NH_3,in}}{a_0 m_{EG}^* T} + \lambda_2(k),\\
&\lambda_2(N)\\
&= 2\kappa_2(\Theta_{NH_3}^*(N) - \Theta_{NH_3}(N)).
\end{aligned} \tag{24}$$

### 2) DISTRIBUTED ENGINE AND UREA-SCR SYSTEM CONTROL

For evaluating the performance of the integrated engine and urea-SCR system status controller, a distributed controller for the engine and urea-SCR system is designed, as shown in Fig. 6. The distributed controller is designed that applies a DDMPC controller [24] for fuel injection and a NMPC controller for $NH_3$ dosing.

For the subspace identification of the DDMPC controller, the data ($\dot{m}_\varphi$, $\omega_e$ and $\mathcal{T}_e$) are derived from the calibration data (shown in Fig. 2 and Fig. 3) for the simplified engine model (3). In this engine optimization problem, the state is selected as $\hat{\mathcal{T}}_{ef}$, and the objective is to find the control policy $\dot{m}_\varphi$ for tracking the optimal torque requirements $\mathcal{T}_e^*$ and reducing the fuel consumption $\dot{m}_\varphi$. The optimization problem for the DDMPC controller can be summarized as shown in equation (25).

$$\begin{aligned}
&\min J_3 = \Gamma_T(\mathcal{T}_e^* - \hat{\mathcal{T}}_{ef})^2 + \Gamma_m(\gamma_f \dot{m}_\varphi)^2,\\
&s.t.\ \hat{\mathcal{T}}_{ef} = L_w w_p + L_u u_f,
\end{aligned} \tag{25}$$

where $u_f$ is the prediction part of $\dot{m}_\varphi$, $w_p$ is the past part of the input data ($\dot{m}_\varphi$ and $\omega_e$) and output data ($\mathcal{T}_e$), and $L_w$ and $L_u$ are the prediction matrices for subspace identification. $\Gamma_T$ and $\Gamma_m$ denote the weight of each part of the function.

In this urea-SCR system optimization problem, the state is selected as $\Theta_{NH_3}$, and the objective is to find the control policy $n_{NH_3,in}$ for tracking the optimal ammonia coverage profile $\Theta_{NH_3}^*$. The optimization problem for the urea-SCR system NMPC controller is simply described as equation (26).

$$\begin{aligned}
&\min J_4 = \varphi_4(\Theta_{NH_3}(t+\Delta\tau)) + \int_t^{t+\Delta\tau} L_4(\Theta_{NH_3}, t')dt',\\
&s.t.\ \dot{\Theta}_{NH_3}(t) = \frac{1}{c_s}[a_2(T_{SCR})(1-\Theta_{NH_3}(t))\frac{n_{NH_3,in}(t)}{a_0 m_{EG}^*(t) T_{SCR}}\\
&\qquad - [a_3(T_{SCR}) + a_4(T_{SCR})C_{NO_x} + a_5(T_{SCR})]\Theta_{NH_3}(t)],
\end{aligned} \tag{26}$$

where $L_4(\Theta_{NH_3}, t') = (\Theta_{NH_3}^*(t) - \Theta_{NH_3}(t))^2$, $\varphi_4(\Theta_{NH_3}(t+\Delta\tau)) = (\Theta_{NH_3}^*(t+\Delta\tau) - \Theta_{NH_3}(t+\Delta\tau))^2$. The solution process for this optimization problem is the same as the above solution processes of the problems (7) and (17).

## IV. EVALUATION OF THE SEQUENTIAL OPTIMIZATION CONTROL SYSTEM

In this section, several simulations are conducted to demonstrate the validity of the proposed sequential optimization control method. An accurate co-simulation model for controller verification is established in the GT-suite/MATLAB environment. The solution result of the optimization problem (19) and the performance of the eco-driving controller are estimated. A calibration process of the estimation model for the ammonia coverage ratio target $\Theta_{NH_3}^*$ is presented. Representative comparison results of performance between the integrated controller (20) and the distributed controller (25) and (26) are presented, and the principles for adjusting the parameters of the integrated controller are discussed.

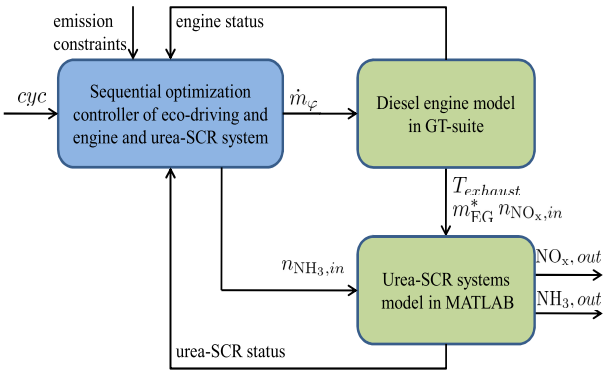


**FIGURE 7.** Co-simulation model of the sequential optimization control in the GT-suite/MATLAB environment.

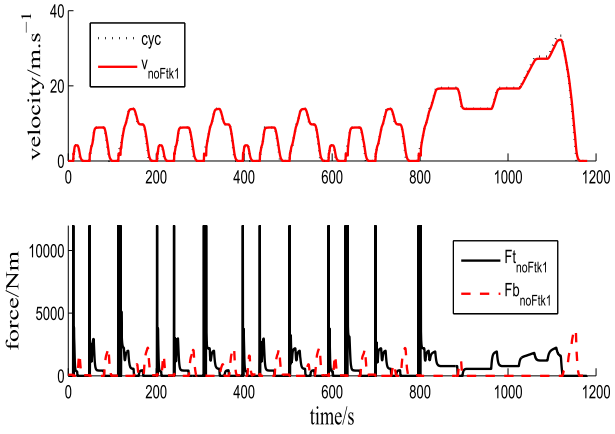


**FIGURE 8.** Performance of the non-optimized controller.

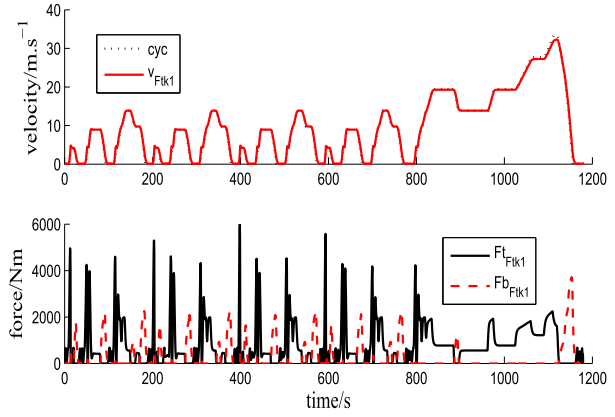


**FIGURE 9.** Performance of the proposed optimized controller.

### A. CO-SIMULATION MODEL IN GT-SUITE/MATLAB ENVIRONMENT

A schematic diagram of the signal transmission between the models and the controllers is shown in Fig. 7. The engine model, as implemented in GT-suite software, is a light-duty diesel engine equipped with a common-rail fuel injection system, a turbocharger system, an intake air cooling system and a urea-SCR system. The engine has four cylinders, a displacement of 2 L and a maximum speed of 4000 r/min. The urea-SCR system model is established in MATLAB software and can accurately describe the actual dynamics of the urea-SCR system [9]. This paper assumes that the cloud-based route optimization system have provided the vehicle velocity profile for the next 3 s at time $t$. In the eco-driving controller, the sampling time is $\Delta\tau = 0.5$ s, and the predictive horizon is $N = 6$. In the integrated engine and urea-SCR system controller, the sampling time is $\Delta t = 50$ ms, and the predictive horizon is $n = 10$.

### B. PERFORMANCE OF THE ECO-DRIVING CONTROLLER

In this paper, the new European driving cycle (NEDC) is adopted as the vehicle velocity profile to be tracked by the controllers to facilitate the evaluation of fuel economy and PM emission. The main parameter values of the proposed optimized controller (19) need to be calibrated. The adjustment principle of these parameters ($\omega_t, \omega_b, \omega_d$ and $\omega_v$) generally prioritizes normalization and then adjusts the proportion according to the control effect. The value of $\kappa_1$ is adjusted according to the value of $\lambda_1$.

The performance results of the non-optimized controller (the cost function $L_1(v(k), F_t(k), F_b(k))$ without $\omega_d(F_t(k+1) - F_t(k))^2$) and the proposed optimized controller are shown in Fig. 8 and Fig. 9, respectively. Both controllers can complete the trajectory tracking control of the NEDC cycle. Compared with the proposed optimized control strategy, the non-optimized controller performs worse. The average peak driving force $Ft_{noFtk1}$ and peak braking force $Fb_{noFtk1}$ of the non-optimized controller are approximately 12000 Nm and 2200 Nm, respectively. The average peak driving force $Ft_{Ftk1}$ and peak braking force $Fb_{Ftk1}$ of the proposed optimized controller are approximately 5000 Nm and 2000 Nm, respectively. Owing to the use of the cost function $L_1(v(k), F_t(k), F_b(k))$ without $\omega_d(F_t(k+1) - F_t(k))^2$, the signals of $Ft_{noFtk1}$ and $Fb_{noFtk1}$ of the non-optimized controller are obviously higher, resulting in a larger energy loss. The fuel analysis result for the distributed engine controller (designed in Section (III-C.2)) show that the fuel consumption of the non-optimized controller is 1652 g, and the fuel consumption of the proposed optimized controller is 1564 g, with a 5.3% improvement in fuel consumption. However, for the proposed optimized controller, during the acceleration process, the vehicle velocity signal $v_{noFtk1}$ shows some slight turning points of secondary acceleration. These features are very obvious at approximately the 50th second, 120th second, 250th second, 310th second, 440th second, 510th second and so forth moments, as shown in Fig. 10.

A comparison of the PM emissions for the non-optimized controller and the proposed optimized controller is shown in Fig. 11. As implemented through the gearbox and the distributed engine controller, the PM emissions of the two driving controllers are also different. Compared with the results of the proposed optimized strategy, the PM emission signal of the non-optimized controller is obviously higher during the acceleration process. In particular, at the 50-70 s phase,

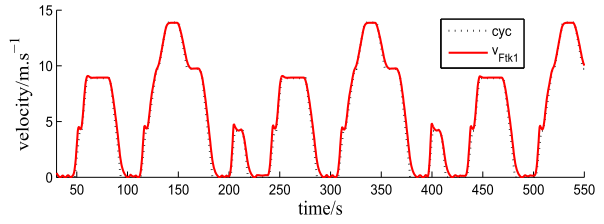


**FIGURE 10.** Zoom in of Fig.6.

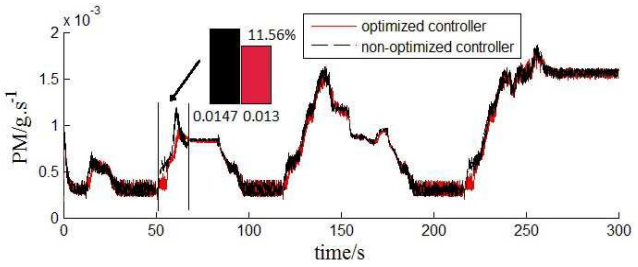


**FIGURE 11.** Performance comparison of PM emission between the non-optimized and optimized controllers.

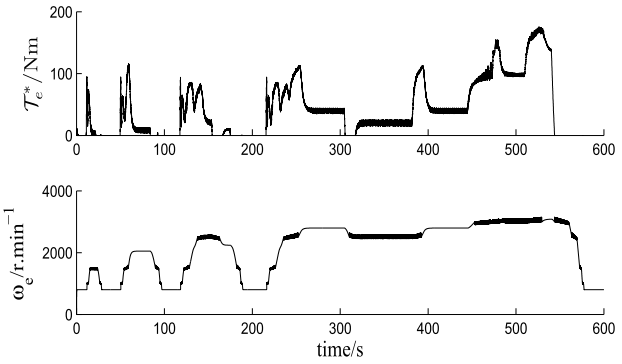


**FIGURE 12.** Engine torque and speed under eco-driving control.

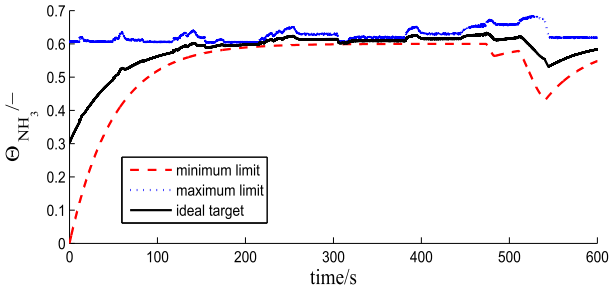


**FIGURE 13.** Estimation result of the ammonia coverage ratio target.

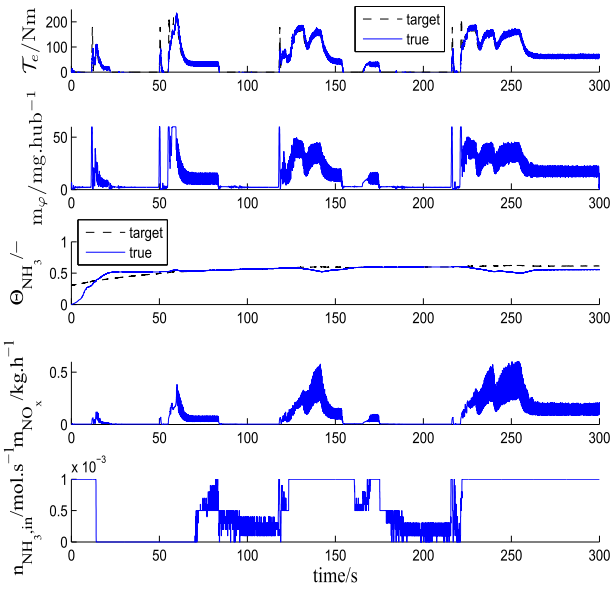


**FIGURE 14.** Performance of the distributed engine and urea-SCR system controller.

the total PM emissions of the non-optimized controller and the proposed optimized controller are 0.0147 $g$ and 0.013 $g$, respectively. The PM emission of the proposed optimized controller is 11.56% lower than that of the non-optimized controller during the moment.

### C. CALIBRATION RESULTS OF THE ESTIMATION MODEL FOR THE AMMONIA COVERAGE RATIO TARGET

With the procedure shown in Fig. 4, the estimation process of the ammonia coverage rate target $\Theta^*_{NH_3}$ is implemented. First, the optimal driving force $F_t^* = Ft_{Ftk1}$ and the actual vehicle velocity $v = v_{Ftk1}$ (as shown in Fig. 9) are obtained by solving the velocity tracking problem. Second, $F_t^*$ and $v$ (the final 600 s part of the NEDC cycle) are respectively converted into the engine torque requirements $\mathcal{T}_e^*$ and engine speed $\omega_e$ through the gearbox, as shown in Fig. 12. Third, all input parameters required for the urea-SCR system operation, including $m_{NO_x}$, $T_{exhaust}$ and $m^*_{EG}$, can be obtained by the calibration relationships shown in equation (3) and the parameters in Table 4 of Appendix Section V.

Fourth, the desired ammonia coverage ratio regions and the ideal target $\Theta^*_{NH_3}$ provided by the estimation model (15) are demonstrated, as shown in Fig. 13. If the actual $\Theta_{NH_3}$ stays in the desired region over the test cycle, both the $NO_x$ emission and ammonia slip requirements can be satisfied. However, during the high load phase of engine operation, the region between $\Theta_{NH_3,low}$ and $\Theta_{NH_3,upp}$ is relatively narrow. Therefore, it is more difficult to control $\Theta_{NH_3}$ at this phase.

### D. COMPARISON RESULTS OF THE PERFORMANCES BETWEEN THE INTEGRATED CONTROLLER AND THE DISTRIBUTED CONTROLLER

The control effectiveness of the distributed engine and urea-SCR system controller and the integrated controller with the parameter $\phi_m$ taking 0.05 are compared in Fig. 14 and Fig. 15, respectively. For the integrated controller, the main parameter values of the equation (20) need to be calibrated. The adjustment principle of these parameters ($\phi_\theta$ and $\phi_T$) generally prioritizes normalization and then adjusts the proportion according to the control effectiveness. The values of $\kappa_2$ and $\kappa_3$ are adjusted according to the value of $\lambda_2$.

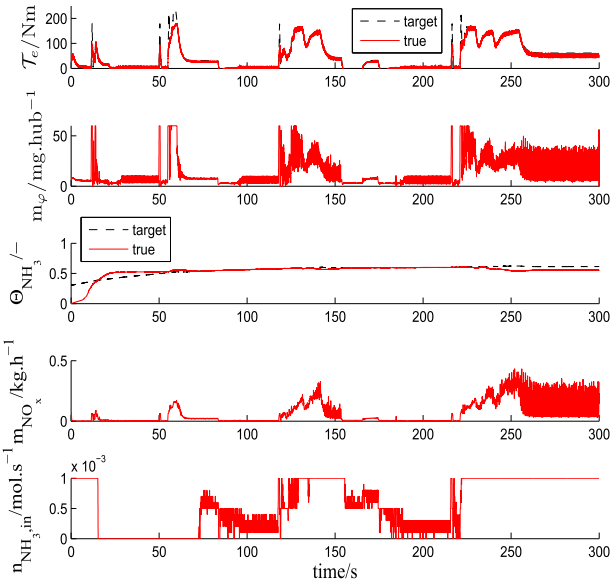


**FIGURE 15.** Performance of the integrated engine and urea-SCR system controller ($\phi_m = 0.05$).

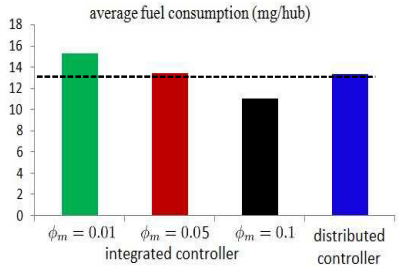


**FIGURE 16.** Performance comparison for total fuel consumption.

The distributed controller and the integrated controller can both efficiently implement the tracking control task. When the torque demand is higher, especially at approximately the 120-150 and 220-260 s phases, the fuel injection mass is increased, resulting a sufficiently high engine $NO_x$ output $m_{NO_x}$ that the $NH_3$ dosing $n_{NH_3,in}$ is fully open. However, the actual ammonia coverage ratio $\Theta_{NH_3}$ decreases, and its deviation from the target value has increased. This result is due to the rapid increases of the chemical reaction between $NO_x$ and adsorbed $NH_3$ and the insufficient maximum capacity of $n_{NH_3,in}$. At approximately the 80-120 and 180-220 s phases, the signal of $n_{NH_3,in}$ fluctuates severely to complete its tracking control.

The comparison results of the average fuel consumption and total $NO_x$ emissions of the engine between the distributed controller and the proposed integrated controller are shown in Fig. 16 and Fig. 17, respectively. As the parameter $\phi_m$ changes from small to large (0.01, 0.05 and 0.1), the average fuel consumption is gradually reduced, which also leads to a reduction in total $NO_x$ emission. However, when the parameter takes the value 0.1, the torque tracking tasks for $\mathcal{T}_e^*$ cannot be performed very well because the excessive increase in

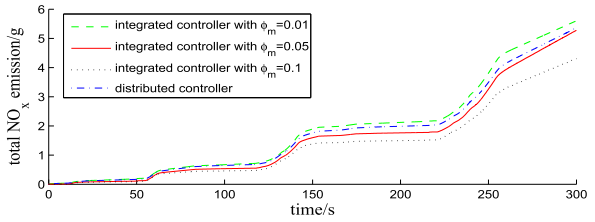


**FIGURE 17.** Performance comparison for total engine $NO_x$ emission.

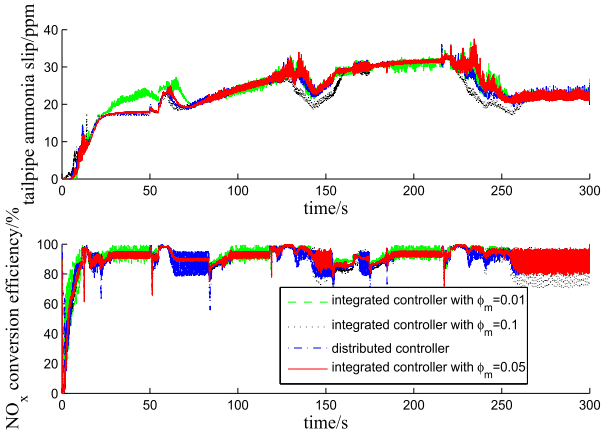


**FIGURE 18.** Performance comparison for the $NH_3$ slip and $NO_x$ conversion efficiency of the urea-SCR system.

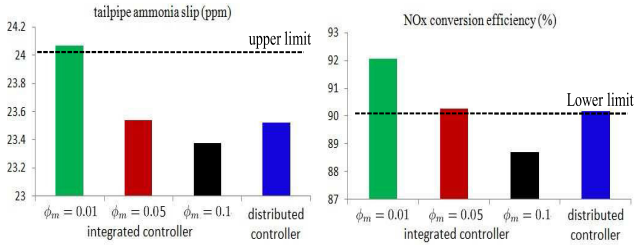


**FIGURE 19.** Performance comparison for the $NH_3$ slip and $NO_x$ conversion efficiency on average.

the parameter $\phi_m$ suppresses the torque tracking control item $\phi_T(\mathcal{T}_e^*(t) - \mathcal{T}_e(t))$. Compared to the distributed controller, the average fuel consumption and total $NO_x$ emission of the proposed integrated controller with $\phi_m = 0.05$ are almost the same.

Through the redox reactions in the urea-SCR system, the final emission effectiveness of $NO_x$ and $NH_3$ is further stabilized, as shown in Fig. 18. Every controller can nearly satisfy the emission requirements by adjusting $n_{NH_3,in}$. As shown in Fig. 19, when $\phi_m = 0.05$, the tailpipe ammonia slip and $NO_x$ conversion efficiency of the integrated controller are respectively 23.54 ppm and 90.29% on average. When the parameter $\phi_m$ takes the value 0.1, both the tailpipe ammonia slip and the $NO_x$ conversion efficiency of the integrated controller are lowest. This is because the excessive increase in the parameter suppresses the item $\phi_\theta(\Theta^*_{NH_3}(t) - \Theta_{NH_3}(t))^2$ tracking $\Theta^*_{NH_3}$. This results in a substantially

**TABLE 4. Calibration parameters of the engine.**

| symbol | value |
|---|---|
| $b_1$ | 2.3962e-5 |
| $b_2$ | -0.5789 |
| $b_3$ | 0.0319 |
| $b_4$ | -0.0204 |
| $b_5$ | 0.00067 |
| $b_6$ | 403.3523 |
| $b_7$ | 3.5321e-5 |
| $b_8$ | -0.0189 |

**TABLE 5. Computational time (s) of the algorithm.**

| algorithm | | average | max |
|---|---|---|---|
| integrated controller ($\phi_m = 0.05$) | | 0.0252 | 0.0472 |
| distributed controller | fuel injection | 0.0101 | 0.0232 |
| | $NH_3$ dosing | 0.0213 | 0.0336 |

reduced amount of $n_{\mathrm{NH_3},in}$ such that the tailpipe ammonia slip and $NO_x$ conversion efficiency are lowest. For the distributed controller, the tailpipe ammonia slip and $NO_x$ conversion efficiency are respectively 23.52 ppm and 90.19% on average, which are almost as good as the results of the integrated controller with $\phi_m = 0.05$. Thus, when the parameter $\phi_m$ is taken as 0.05, the two emission performances of the integrated controller remain better balanced.

The simulations were run on an Intel(R) Core(TM) i7-4790 CPU (3.60GHz), and an estimate of the CPU computational time was obtained using a MATLAB command. The computational time of each algorithm in a single sampling period is shown in Table 5 of Appendix Section V. Compared to the fuel injection DDMPC of the distributed controller, the urea dosing NMPC requires a longer computational time. Compared to the urea dosing NMPC, the integrated controller with $\phi_m = 0.05$ requires 15.47% more computational time on average. With hard-ware computing power expected only to increase, this disadvantage of the integrated controller will at some point become negligible.

## V. CONCLUSION

In this paper, a sequential optimization control method with three stages is designed to simplify the moving horizon optimization problem for eco-driving taking into account fuel economy and emissions. Simulations are conducted to demonstrate the validity of the proposed optimization problem solved under the PMP framework. In stage I, compared with the non-optimized controller for the vehicle velocity tracking problem, the proposed optimized control strategy can simultaneously achieve high fuel efficiency and low PM emissions. In stage III, to implement the driving force requirement and ammonia coverage ratio target, an integrated engine and urea-SCR system controller and a distributed controller are proposed. The fuel consumption and emissions of the integrated controller can be improved to match those of the distributed method through parameter adjustment. However, the integrated controller requires 15.47% higher computational time on average. Overall, with hard-ware computing power expected only to increase, the sequential optimization controller proposed is concluded to be beneficial for application under RDE conditions.

## APPENDIX

See Tables 4 and 5.

## REFERENCES

[1] K. Jiang, H. Zhang, and J. Lin, "$NH_3$ coverage ratio estimation of diesel-engine SCR systems by a dual time-scale extended Kalman filter," *IEEE Trans. Veh. Technol.*, vol. 67, no. 4, pp. 3625–3629, Apr. 2017.

[2] T. V. Johnson, "Review of diesel emissions and control," *Int. J. Engine Res.*, vol. 10, no. 5, pp. 275–285, 2010.

[3] P. Chen and J. Wang, "Nonlinear model predictive control of integrated diesel engine and selective catalytic reduction system for simultaneous fuel economy improvement and emissions reduction," *J. Dyn. Syst. Meas. Control*, vol. 137, no. 8, 2015, Art. no. 081008.

[4] J. Zhao, X. Gong, Y. Hu, J. Gao, and H. Chen, "An ammonia coverage ratio observing and tracking controller: Stability analysis and simulation evaluation," *Sci. China Inf. Sci.*, vol. 62, Jun. 2019, Art. no. 062201.

[5] Y. Sun, W. Dong, and X. Yu, "Effects of coolant temperature coupled with controlling strategies on particulate number emissions in GDI engine under idle stage," *Fuel*, vol. 225, no. 5, pp. 1–9, 2018.

[6] M. Devarakonda, G. Parker, J. H. Johnson, and V. Strots, "Model-based control system design in a urea-SCR aftertreatment system based on $NH_3$ sensor feedback," *Int. J. Automot. Technol.*, vol. 10, no. 6, pp. 653–662, 2009.

[7] B. Yang, L. Keqiang, H. Ukawa, and M. Handa, "Modelling and control of a non-linear dynamic system for heavy-duty trucks," *Proc. Inst. Mech. Eng., D, J. Automobile Eng.*, vol. 220, no. 10, pp. 1423–1435, 2006.

[8] M.-F. Hsieh, J. Wang, and M. Canova, "Two-level nonlinear model predictive control for lean $NO_x$ trap regenerations," *J. Dyn. Syst., Meas., Control*, vol. 132, no. 4, 2010, Art. no. 041001.

[9] J. Zhao, Y. Hu, X. Gong, and H. Chen, "Modelling and control of urea-SCR systems through the triple-step non-linear method in consideration of time-varying parameters and reference dynamics," *Trans. Inst. Meas. Control*, vol. 40, no. 1, pp. 287–302, 2018.

[10] H. Zhang, P. Chen, J. Wang, and Y.-Y. Wang, "Integrated study of inland-vessel diesel engine two-cell SCR systems with dynamic references," *IEEE/ASME Trans. Mechatronics*, vol. 22, no. 3, pp. 1195–1206, Jun. 2017.

[11] R. You, M. Meng, J. Zhang, L. Zheng, T. Hu, and X. Li, "A noble-metal-free SCR-LNT coupled catalytic system used for high-concentration $NO_x$ reduction under lean-burn condition," *Catal. Today*, vol. 327, pp. 347–356, May 2019.

[12] G. Wu, K. Boriboonsomsin, and M. J. Barth, "Development and evaluation of an intelligent energy-management strategy for plug-in hybrid electric vehicles," *IEEE Trans. Intell. Transp. Syst.*, vol. 15, no. 3, pp. 1091–1100, Jun. 2014.

[13] T. S. Kim, C. Manzie, and R. Sharma, "Model predictive control of velocity and torque split in a parallel hybrid vehicle," in *Proc. IEEE Int. Conf. Syst., Man Cybern.*, Oct. 2009, pp. 2014–2019.

[14] L. L. Guo, B. Gao, Y. Gao, and H. Chen, "Optimal energy management for HEVs in eco-driving applications using bi-level MPC," *IEEE Trans. Intell. Transp. Syst.*, vol. 18, no. 8, pp. 2153–2162, Aug. 2017.

[15] H. Chen and C. W. Scherer, "Moving horizon $\mathcal{H}_\infty$ control with performance adaptation for constrained linear systems," *Automatica*, vol. 42, no. 6, pp. 1033–1040, 2006.

[16] Y. Ma and J. Wang, "Integrated power management and aftertreatment system control for hybrid electric vehicles with road grade preview," *IEEE Trans. Veh. Technol.*, vol. 66, no. 12, pp. 10935–10945, Dec. 2017.

[17] A. Bonfils, Y. Creff, O. Lepreux, and N. Petit, "Closed-loop control of a SCR system using a $NO_x$ sensor cross-sensitive to $NH_3$," *J. Process Control*, vol. 24, no. 2, pp. 368–378, 2014.

[18] A. Sciarretta, G. De Nunzio, and L. L. Ojeda, "Optimal ecodriving control: Energy-efficient driving of road vehicles as an optimal control problem," *IEEE Control Syst.*, vol. 35, no. 5, pp. 71–90, Oct. 2015.
[19] X. Gong, I. Kolmanovsky, E. Garone, K. Zaseck, and H. Chen, "Constrained control of free piston engine generator based on implicit reference governor," *Sci. China Inf. Sci.*, vol. 61, no. 7, pp. 70203-1–70203-16, 2018.
[20] T. Van Keulen, J. Gillot, B. De Jager, and M. Steinbuch, "Solution for state constrained optimal control problems applied to power split control for hybrid vehicles," *Automatica*, vol. 50, no. 1, pp. 187–192, 2014.
[21] H. Chu, L. Guo, B. Gao, H. Chen, N. Bian, and J. Zhou, "Predictive cruise control using high-definition map and real vehicle implementation," *IEEE Trans. Veh. Technol.*, vol. 67, no. 12, pp. 11377–11389, Dec. 2018.
[22] M.-F. Hsieh and J. Wang, "A two-cell backstepping-based control strategy for diesel engine selective catalytic reduction systems," *IEEE Trans. Control Syst. Technol.*, vol. 19, no. 6, pp. 1504–1515, Nov. 2011.
[23] J. Zhao, S. Zhou, Y. Hu, M. Ju, R. Ren, and H. Chen, "Open-source dataset for control-oriented modelling in diesel engines," *Sci. China Inf. Sci.*, vol. 62, no. 7, 2019, Art. no. 027101.
[24] X. Lu, H. Chen, P. Wang, and B. Gao, "Design of a data-driven predictive controller for start-up process of AMT vehicles," *IEEE Trans. Neural Netw.*, vol. 22, no. 12, pp. 2201–2212, Dec. 2011.
[25] C. M. Schär, C. H. Onder, and H. P. Geering, "Control of an SCR catalytic converter system for a mobile heavy-duty application," *IEEE Trans. Control Syst. Technol.*, vol. 14, no. 4, pp. 641–653, Jul. 2006.
[26] M. L. Heiredal, A. D. Jensen, J. R. Thøgersen, F. J. Frandsen, and J.-U. Friemann, "Pilot-scale investigation and CFD modeling of particle deposition in low-dust monolithic SCR DeNO$_x$ catalysts," *AIChE J.*, vol. 59, no. 6, pp. 1919–1933, 2013.
[27] P. Chen and J. Wang, "Coordinated active thermal management and SCR control for simultaneous fuel economy improvement and emissions reduction during low-temperature operations," *J. Dyn. Syst. Meas. Control*, vol. 137, no. 12, pp. 634–641, 2015.

**JINGHUA ZHAO** received the M.S. degree in software engineering from the Harbin Institute of Technology, Harbin, China, in 2008, and the Ph.D. degree in power machinery and engineering from Jilin University, Changchun, China, in 2012, where he holds a Postdoctoral position. He is currently an Associate Professor with the Computer College, Jilin Normal University. His current research interests include nonlinear control and automotive control.

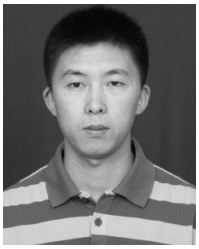

**YUNFENG HU** received the M.S. degree in basic mathematics and the Ph.D. degree in control theory and control engineering from Jilin University, Changchun, China, in 2008 and 2012, respectively, where he is currently an Associate Professor with the Department of Control Science and Engineering. His current research interests include nonlinear control and automotive control.

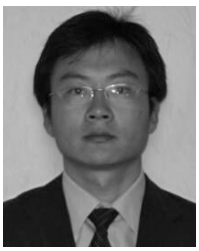

**BINGZHAO GAO** received the B.S. and M.S. degrees in vehicle engineering from Jilin University, Changchun, China, in 1998 and 2002, respectively, and the Ph.D. degrees in mechanical engineering from Yokohama National University, Yokohama, Japan, and in control engineering from Jilin University, in 2009. He is currently a Professor with Jilin University. His current research interests include vehicle powertrain control and vehicle stability control.